PHYSICAL REVIEW B VOLUME 41, NUMBER 11 15 APRIL 1990-I

Anharmonic lattice vibrations in noble metals

M. Zoli*
Dipartimento di Fisica, Università degli Studi di Modena, via Campi 213A, I-41100 Modena, Italy

(Received 6 October 1989)

Both macroscopic and microscopic effects of anharmonicity in noble metals have been calculated in low-order perturbation theory. A strain-dependent Helmholtz free energy is used to evaluate the thermoelastic properties. The interactions are modeled according to a force-constant scheme which includes angular forces in the harmonic part of the potential. The cubic and quartic anharmonic force constants are related to third- and fourth-order elastic constants. It is shown that the cubic pairwise interactions have to be extended up to the third-neighbor shell, in order to fit experiments in Ag and Au. A slightly negative anharmonic contribution to the constant-volume specific heat is found, in good agreement with recent experimental inquiries. Phonon line shifts are computed along the high-symmetry directions of the Brillouin zone. Our results reproduce well neutron-scattering measurements which are available for copper at high temperatures. An enhanced line shift in longitudinal phonons of noble metals, along the $[\xi 0 0]$ direction, is pointed out.

I. INTRODUCTION

The microscopic effects of anharmonicity in solids are displayed in the temperature dependence of the phonon normal modes of vibration. At the lowest order, the anharmonic contributions can be represented by shifts Δ_T,

$$\Delta_T = \Delta^{(0)} + \Delta^{(3)} + \Delta^{(4)} ,$$

in the harmonic frequencies. The term $\Delta^{(0)}$ is proportional to the thermal expansion of the crystal,[1] while $\Delta^{(3)}$ and $\Delta^{(4)}$ can be determined, at a fixed volume, in the framework of perturbation theory:[2] $\Delta^{(4)}$ is the first-order term and $\Delta^{(3)}$ is the lowest second-order term, in the real part of the phonon self-energy. Higher-order corrections are relevant for rare-gas solids[3,4] even at temperatures $T \simeq \frac{1}{3} T_m$ (where T_m is the melting temperature) and a variational procedure employing the Bogoliubov's inequality[5] (self-consistent phonon method) has to be adopted[6] to determine the effective T dependence of the phonon frequencies. It has also been argued[7] that such higher-order corrections should be small in metals. The interatomic potentials have, in metals, much less steep repulsive cores than potentials in rare-gas crystals. As a consequence, the nth order ($n \geq 3$) derivatives of the potential, which determine anharmonicity, are in metals much smaller than in rare-gas crystals. Besides, the structure-independent electron gas gives rise, in metals, to large cohesive forces. On the other hand, some authors[8,9] have suggested that higher-order effects are relevant, for alkali metals, at $T \simeq T_m$, so that the lowest-order perturbation theory does not hold near the melting point. In any case, being the melting temperature of metals between about $2\Theta_D$ and $8\Theta_D$ (Θ_D is the Debye temperature), one notes that metals still present wide ranges of temperatures in which microscopic anharmonic effects can be handled within the lowest-order perturbation theory.[10]

Once the shifts Δ_T are known, the macroscopic manifestations of anharmonicity can also be predicted: Barron[11] has shown that the anharmonic effects in thermodynamics are, to lowest order, correctly accounted for if the harmonic frequencies are shifted by Δ_T in the harmonic entropy formula. Furthermore, Hui and Allen[12] have conjectured that once the temperature-dependent experimental phonon frequencies are inserted in the harmonic entropy formula, then the anharmonic effects are included to a higher order of approximation. This simple replacement is not valid for other thermodynamic functions such as free energy and internal energy.

In our previous paper,[13] the thermodynamic of Cu and Al was extensively investigated. We adopted a general approach[14] which allows for an explicit volume dependence of the Helmholtz free energy. The interatomic potential was modeled according to a force-constant scheme which includes nearest-neighbor central interactions in the anharmonic tail. It was shown that the quasiharmonic approximation is successful in the evaluation of the thermoelastic properties. Anharmonic lattice vibration contributions to constant-volume specific heat were exactly calculated, to the lowest order, and found to be slightly negative, at room temperature, for both metals. This result lends support to recent accurate experimental inquiries.[15]

In this paper, the anharmonic properties of the other two noble metals, Ag and Au, will be addressed. In Sec. II, the linear coefficient of thermal expansion and the thermodynamic Grüneisen parameter are evaluated within the theoretical framework described in Ref. 13. The calculations are based on a force-constant-model potential. The harmonic part of the potential takes into account central forces up to the fourth-neighbor shell, plus first-neighbor three-body forces which avoid the fulfillment of the second-order Cauchy relations. It is shown that a simple first-neighbor anharmonic potential does not suffice for these metals, so that the cubic central interactions have to be extended up to third neighbors in order to fit experimental data. In Sec. III, the shifts Δ_T

in the harmonic frequencies of Cu, Ag, and Au are exactly computed; for copper, comparisons are made with available neutron-scattering measurements[16] along the high-symmetry directions of the Brillouin zone. In Sec. IV, the renormalized phonon frequencies (at constant volume) are inserted in the harmonic entropy formula, and the anharmonic contributions to constant-volume specific heat are evaluated. In Sec. V, the conclusions are drawn.

II. THERMOELASTIC PROPERTIES

The volume dependence of the Helmholtz free energy $F(V,T)$ is the key ingredient in the analyses of the thermoelastic properties of metals.[17] If a homogeneous deformation is applied to the crystal, the phonon-displacement field can be written[14] as a superposition of microscopic atomic vibrations inside the unitary cell and macroscopic deformations of the cell itself. In this way, the effects of strain on the atomic-mean positions are automatically introduced in the crystal Hamiltonian. The full set of equations which relates the strain Hamiltonian H_S to the atomic force-constant tensors are reported in Ref. 13. Here, we only remember that, by applying the linked-cluster theorem,[18] the perturbative term $F_1(V,T)$ in the Helmholtz free energy is given by

$$F_1=\beta^{-1}\left\langle T_\tau\left[\int_0^\beta d\tau_1 H_S(\tau_1)-\frac{1}{2}\int_0^\beta d\tau_1\int_0^\beta d\tau_2 H_S(\tau_1)H_S(\tau_2)\right]S(\beta)\right\rangle_{0,\mathrm{conn}} \tag{1}$$

with

$$S(\beta)=1-\int_0^\beta d\tau' H_{\mathrm{anh}}(\tau') , \tag{2}$$

β is the inverse temperature, H_{anh} is the pure anharmonic Hamiltonian made of the cubic and quartic terms in the phonon normal coordinates, $\langle \cdots \rangle_{0,\mathrm{conn}}$ denotes that quantum averages are made on the unperturbed eigenstates of the crystal Hamiltonian and only connected diagrams must be retained. Thermal averages are implied by the formalism. From Eq. (1), the temperature dependence of the following properties can be easily derived.

(a) Stress tensor $\sigma_{\alpha\beta}$

$$V\sigma_{\alpha\beta}(T)=\left[\frac{\partial F_1}{\partial \eta_{\alpha\beta}}\right]_0 . \tag{3}$$

V is the crystal volume in the undeformed state, $\eta_{\alpha\beta}$ is the strain tensor which vanishes for pure rotations.

(b) Isothermal second-order elastic constants $C^T_{\alpha\beta\alpha'\beta'}$

$$VC^T_{\alpha\beta\alpha'\beta'}(T)=\left[\frac{\partial^2 F_1}{\partial\eta_{\alpha\beta}\partial\eta_{\alpha'\beta'}}\right]_0 . \tag{4}$$

(c) Linear coefficient of thermal expansion α

$$\alpha(T)=-\frac{1}{B^T(T)}\left[\frac{\partial\sigma_{11}}{\partial T}\right]_0 , \tag{5}$$

where $B^T(T)$ is the isothermal bulk modulus computed on the base of Eq. (4).

The lowest-order diagrams which contribute to the stress tensor and elastic constants are shown in Fig. 1. Their analytic expressions are reported in Ref. 13 and are not given here. Higher-order diagrams, involving H_{anh} in Eq. (2), have also been evaluated, but their contribution to the thermoelastic properties of noble metals is found to be negligible (3 orders of magnitude smaller than $D3$ in Fig. 1), even near the melting temperature. Therefore, the quasiharmonic approximation [which corresponds to retain only the diagrams in Fig. 1 (Ref. 14)] works satisfactorily insofar as thermoelastic properties are concerned. As already seen in the case of copper,[13] the investigation of Ag and Au also reveals that the values of the diagrams $D1$ and $D2$ are scarcely relevant in comparison with the values of the diagram $D3$. As a consequence, the effects of the quartic force-constant tensor can be dropped.

The cubic anharmonic potential is built up according to a force-constant model. By equating the vibrational energy density and the elastic energy density of a strained crystal, general relations between the cubic force constants and the third-order elastic constants are derived. The anharmonic central interactions have been extended up to the third-neighbor shell. The full set of equations is reported in Appendix A. Since the third-order elastic constants are experimentally known,[19] the cubic force constants are easily derived through Eqs. (A6). In Appendix B, the analytic expressions of the thermal pressure

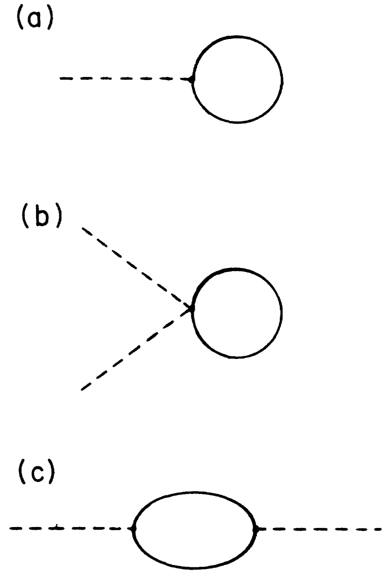

FIG. 1. (a) First-order diagram ($D1$) contributing to the stress tensor. (b) First-order diagram ($D2$) contributing to the second-order elastic constants. (c) Second-order diagram ($D3$) contributing to the second-order elastic constants. The dashed lines are associated with the strain Hamiltonian H_S; the solid lines denote the phonon propagators.

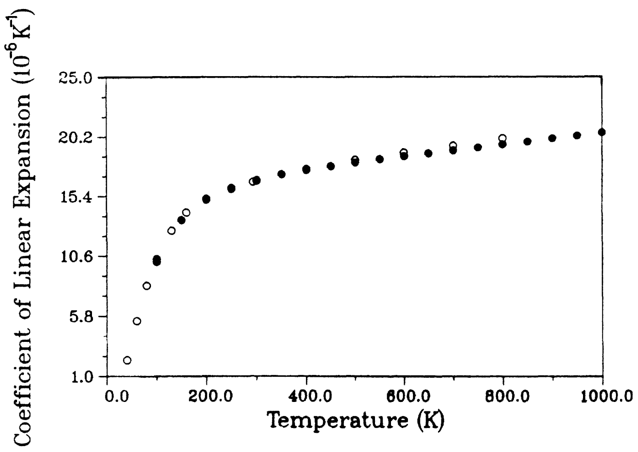

FIG. 2. Linear coefficient of thermal expansion vs temperature in copper. ●, our calculation according to the $1CM$-model potential. ○, experimental data from Ref. 21.

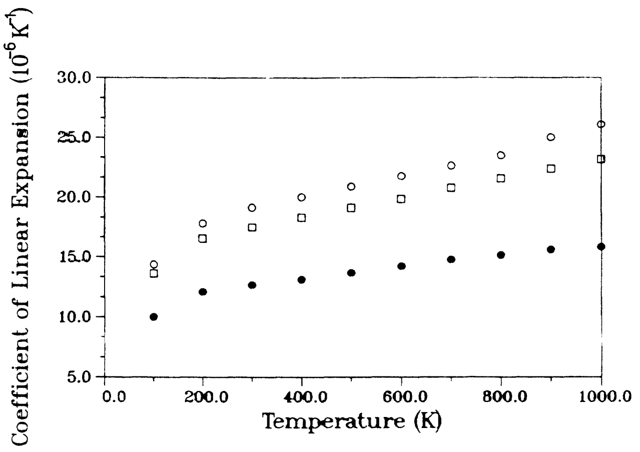

FIG. 3. Linear coefficient of thermal expansion vs temperature in silver. ● our calculation according to the $1CM$-model potential. □, our calculation according to the $3CM$-model potential. ○, experimental data from Ref. 22.

$\alpha \cdot B^T$ and the mode Grüneisen parameter $\gamma(\mathbf{q},j)$, as functions of the cubic force constants, are given in detail. In Figs. 2–4, the linear thermal expansion coefficients α are reported for Cu, Ag, and Au, respectively. Both a first-neighbor cubic potential ($1CM$) and a third-neighbor cubic potential ($3CM$), have been assumed in the calculations.

Figure 2 points out that a short-ranged cubic potential ($1CM$) accurately fits the experimental data in the case of Cu. In Figs. 3 and 4, it is shown that the $1CM$ potential does not suffice, for Ag and Au, and long-range cubic forces ($3CM$) have to be taken into account.

In Table I, the thermodynamic Grüneisen parameters $\gamma_{\rm td}$ of noble metals are given both in the $1CM$ and $3CM$, together with experimental data at room temperature. It is confirmed that the long-range cubic forces give rise to significant improvements in Ag and Au, although the experimental values of Ag are slightly underestimated also by the $3CM$-model potential.

In the next section, the calculated values of thermoelastic properties, namely α and $\gamma(\mathbf{q},j)$, are used to establish the thermal dilation effects on the phonon frequencies.

III. ANHARMONIC FREQUENCY SHIFTS

Due to anharmonicity the frequencies $\omega(\mathbf{q},j)$ of phonons, with wave vector $\mathbf{q}$ and mode index j, are volume and temperature dependent. To lowest order in perturbation theory the harmonic frequencies ω_0 shift to

$$\omega(\mathbf{q},j)=\omega_0(\mathbf{q},j)+\Delta_T(\mathbf{q},j) \tag{6}$$

with

$$\Delta_T(\mathbf{q},j)=\Delta^{(0)}(\mathbf{q},j)+\Delta^{(3)}(\mathbf{q},j)+\Delta^{(4)}(\mathbf{q},j) \ . \tag{7}$$

The shift $\Delta^{(0)}(\mathbf{q},j)$, which accounts for the dilation effects, can be written as

$$\Delta^{(0)}(\mathbf{q},j)=-3\alpha(T)T\gamma(\mathbf{q},j)\omega_0(\mathbf{q},j) \ . \tag{8}$$

$\gamma(\mathbf{q},j)$ is given in Eq. (B3) and $\alpha(T)$ is computed according to the $3CM$-model potential. The terms $\Delta^{(4)}(\mathbf{q},j)$ and $\Delta^{(3)}(\mathbf{q},j)$ are the lowest-order contribution in the real part of the phonon self-energy. They correspond to the diagrams in Figs. 5(a) and 5(b), respectively. Their analytic expressions are

$$\begin{aligned}
\Delta^{(4)}(\mathbf{q},j)&=\frac{12}{\hbar}\sum_{\mathbf{q}_1,j_1} V^{(4)}(\mathbf{q},j;\mathbf{q}_1,j_1;-\mathbf{q}_1,j_1;-\mathbf{q},j)(2n_1+1) \ ,\\
\Delta^{(3)}(\mathbf{q},j)&=-\frac{18}{\hbar^2}\sum_{\mathbf{q}_1,\mathbf{q}_2}\sum_{j_1,j_2}|V^{(3)}(-\mathbf{q},j;\mathbf{q}_1,j_1;\mathbf{q}_2,j_2)|^2\mathrm{P}\left[\frac{n_1+n_2+1}{\omega_0(\mathbf{q},j)+\omega_0(1)+\omega_0(2)}-\frac{n_1+n_2+1}{\omega_0(\mathbf{q},j)-\omega_0(1)-\omega_0(2)}\right.\\
&\qquad\left.+\frac{n_1-n_2}{\omega_0(\mathbf{q},j)-\omega_0(1)+\omega_0(2)}-\frac{n_1-n_2}{\omega_0(\mathbf{q},j)+\omega_0(1)-\omega_0(2)}\right] ,
\end{aligned} \tag{9}$$

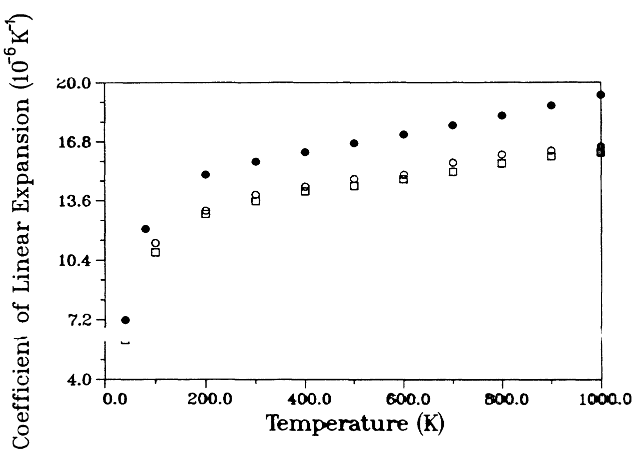

FIG. 4. Linear coefficient of thermal expansion vs temperature in gold. ●, our calculation according to the 1*CM*-model potential. □, our calculation according to the 3*CM*-model potential. ○, experimental data from Ref. 22.

where P denotes the principal value and $\omega_0(i)\equiv\omega_0(\mathbf{q}_i,j_i)$, $n_i\equiv n(\omega_0(i))$ are the Bose-Einstein statistical factors, $V^{(3)}$ and $V^{(4)}$ are the Fourier transforms of the third- and fourth-order force-constant tensors, respectively. The harmonic eigenstates and eigenvalues are computed within our usual force-constant-model potential which includes first-neighbor angular forces.

In calculations of phonon line shift, the quartic anharmonic term, arising from the first-order perturbation theory, has to be considered. We have related the fourth-order force constants to the fourth-order elastic constants. A set of equations which allows one to determine up to three fourth-order parameters, is listed in Appendix A. The evaluation of the fourth-order force constants is complicated by the incomplete availability of experimental values for fourth-order elastic constants. Nonetheless, the leading quartic force constants (Q_1) of noble metals, computed by Eqs. (A7), reasonably agree with the values obtained by fitting the experimental strain derivative of Grüneisen parameter[20] [Eq. (A8)]. Therefore, our force-constants approach should yield a reliable evaluation of quartic anharmonic effects.

We have made numerical calculations of the frequency shift $\Delta_T(\mathbf{q},j)$. The sums over wave vectors [Eqs. (9)] have been evaluated by using 8704 points in the entire Brillouin zone. The adopted representation for the principal value in the second of Eqs. (9) is

$$P\left[\frac{1}{x}\right]=\lim_{\epsilon\to 0}\left[\frac{x}{x^2+\epsilon^2}\right], \tag{10}$$

where, in practice, ϵ must be small but finite. We have found that $\Delta^{(3)}(\mathbf{q},j)$ is sensibly independent of ϵ over a range of values of ϵ. The value which lies in the center of such a range, $\epsilon=0.2$ meV, has been accordingly used. The terms in Eqs. (8) and (9) have been calculated at room temperature, with the wave vector $\mathbf{q}$ lying along the high-symmetry directions of the Brillouin zone. In Tables II–IV, the computed line shifts of longitudinal phonons are presented for Cu, Ag, and Au, respectively. As for Cu, the frequency shifts $\Delta_T(\mathbf{q},j)$ have also been computed at 673 K, to allow a comparison with available high-temperature experimental data.[16] The overall agreement between theory and experiment is quite satisfactory, although the large experimental errors preclude making any definitive statements. The results indicate a general softening of the anharmonic lattices mainly due to the thermal expansion addendum $\Delta^{(0)}$. An examination of

TABLE I. Thermodynamic Grüneisen parameter of noble metals at room temperature. (a) γ_{td} is evaluated according to a first-neighbor ranged anharmonic potential (1*CM*). (b) γ_{td} is evaluated according to a third-neighbor ranged anharmonic potential (3*CM*). (c) The experimental data are taken from Ref. 20.

	γ_{td}(a)	γ_{td}(b)	γ_{td}(c)
Cu	2.019	2.012	2.0
Ag	1.675	2.247	2.4
Au	3.372	2.943	3.0

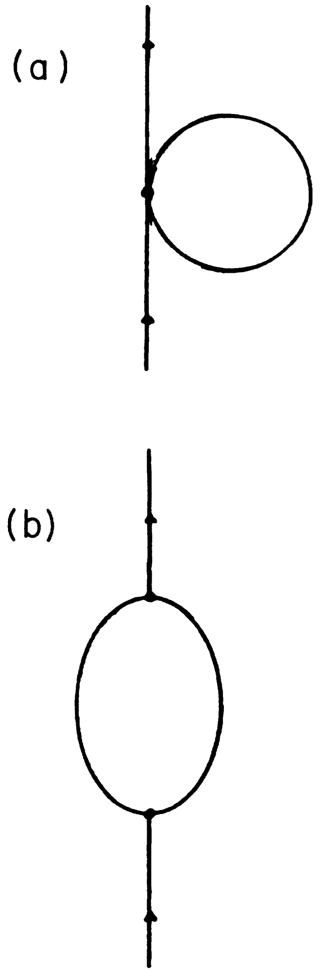

FIG. 5. (a) First-order diagram which contributes to the proper phonon self-energy. (b) Lower second-order diagram which contributes to the proper phonon self-energy.

TABLE II. Line shifts of longitudinal phonons in copper. The shifts are in units meV. The wave vectors are in units $2\pi/a$. $\Delta^{(0)}$ is evaluated from Eq. (8). $\Delta^{(4)}$ and $\Delta^{(3)}$ are evaluated from Eqs. (9). Δ_T, defined in Eq. (7), is calculated at room temperature. $\delta\Delta_T=\Delta_T(673\text{ K})-\Delta_T(300\text{ K})$. (a) The experimental data are taken from Ref. 16.

Wave vector **q**	$\Delta^{(0)}$	$\Delta^{(4)}$	$\Delta^{(3)}$	Δ_T	$\delta\Delta_T$	$\delta\Delta_T^{(a)}$
(0.2,0.0,0.0)	−0.337	0.194	−0.237	−0.379	−0.443	−0.413
(0.4,0.0,0.0)	−0.640	0.370	−0.415	−0.686	−0.587	−0.342
(0.6,0.0,0.0)	−0.898	0.618	−0.730	−1.010	−0.712	−0.56
(0.8,0.0,0.0)	−1.085	0.626	−0.793	−1.251	−1.324	−1.12
(1.0,0.0,0.0)	−1.156	0.667	−0.464	−0.953	−1.008	−1.13
(0.1,0.1,0.1)	−0.339	0.243	−0.233	−0.329		
(0.2,0.2,0.2)	−0.656	0.470	−0.382	−0.569		
(0.3,0.3,0.3)	−0.933	0.667	−0.641	−0.907		
(0.4,0.4,0.4)	−1.132	0.809	−0.634	−0.957		
(0.5,0.5,0.5)	−1.206	0.862	−0.617	−0.960		
(0.15,0.15,0.0)	−0.396	0.272	−0.263	−0.387		
(0.30,0.30,0.0)	−0.732	0.497	−0.469	−0.704		
(0.45,0.45,0.0)	−0.960	0.634	−0.743	−1.069		
(0.60,0.60,0.0)	−1.029	0.844	−0.829	−1.015	−0.921	−0.732
(0.75,0.75,0.0)	−1.056	0.786	−1.061	−1.331	−1.112	−0.948

Tables II–IV reveals that the purely anharmonic terms $\Delta^{(3)}(\mathbf{q},i)$ and $\Delta^{(4)}(\mathbf{q},j)$ often tend to cancel out each other. We point out that a significant asymmetry in the phonon shift takes place along the $[\xi,0,0]$ direction, at $\xi=0.8$ in Cu and Ag, and at $\xi=0.6$ in Au. This interesting feature of longitudinal phonons is produced by the term $\Delta^{(3)}(\mathbf{q},j)$ which is rapidly varying with **q**. An analogous result was found by Koehler *et al.*[23] in aluminum. These authors suggested that a high density of final states has to be expected for the decay process of the longitudinal mode (0.8,0,0). We would also emphasize that, in our previous investigation of anharmonicities,[24] an enhanced phonon linewidth has been found for the longitudinal mode (0.8,0,0) in aluminum and gold.

IV. CONSTANT-VOLUME ANHARMONIC SPECIFIC HEAT

Recent accurate experimental investigations on noble metals[15] have suggested that a negative anharmonic contribution to constant-volume specific heat (ΔC_V^{anh}) is expected at (and below) room temperature. The calculations which we have carried out in Sec. III allow us to address the matter, although quantitative comparisons with experiments are difficult, since ΔC_V^{anh} is not directly observed.

According to the harmonic theory, the entropy function is given by

$$S=-k_B\left[\sum_{\mathbf{q},j}\ln\{1-\exp[-\beta\hbar\omega_0(\mathbf{q},j)]\}-\beta\sum_{\mathbf{q},j}\frac{\hbar\omega_0(\mathbf{q},j)}{\exp[\beta\hbar\omega_0(\mathbf{q},j)]-1}\right], \qquad (11)$$

where K_B is the Boltzmann constant.

Cochran and Cowley[25] have shown that, to leading order in perturbation theory of anharmonicity, the entropy is given correctly by the harmonic formula, with the harmonic frequencies ω_0 replaced by the measurable frequencies. Once this replacement holds, the entropy formula gives a good approximation to the constant-pressure thermodynamics.[11] Such a procedure has been applied to aluminum, lead,[26,27] and niobium.[12]

The general theory of the anharmonic crystal[28,29]

TABLE III. Line shifts of longitudinal phonons in silver at room temperature. See Table II for definitions.

Wave vector	$\Delta^{(0)}$	$\Delta^{(4)}$	$\Delta^{(3)}$	Δ_T
(0.2,0.0,0.0)	−0.292	0.242	−0.180	−0.231
(0.4,0.0,0.0)	−0.568	0.376	−0.305	−0.497
(0.6,0.0,0.0)	−0.803	0.490	−0.529	−0.842
(0.8,0.0,0.0)	−0.966	0.569	−0.757	−1.154
(1.0,0.0,0.0)	−1.025	0.598	−0.460	−0.887
(0.15,0.15,0.0)	−0.351	0.301	−0.206	−0.255
(0.30,0.30,0.0)	−0.650	0.470	−0.338	−0.518
(0.45,0.45,0.0)	−0.851	0.572	−0.546	−0.825
(0.60,0.60,0.0)	−0.915	0.583	−0.744	−1.076
(0.75,0.75,0.0)	−0.934	0.538	−0.880	−1.276

TABLE IV. Line shifts of longitudinal phonons in gold, at room temperature. See Table II for definitions.

Wave vector **q**	$\Delta^{(0)}$	$\Delta^{(4)}$	$\Delta^{(3)}$	Δ_T
(0.2,0.0,0.0)	−0.194	0.142	−0.184	−0.236
(0.4,0.0,0.0)	−0.376	0.181	−0.316	−0.511
(0.6,0.0,0.0)	−0.531	0.214	−0.469	−0.786
(0.8,0.0,0.0)	−0.638	0.237	−0.020	−0.421
(1.0,0.0,0.0)	−0.677	0.246	−0.015	−0.446
(0.15,0.15,0.0)	−0.243	0.282	−0.239	−0.199
(0.30,0.30,0.0)	−0.445	0.347	−0.296	−0.395
(0.45,0.45,0.0)	−0.577	0.379	−0.443	−0.640
(0.60,0.60,0.0)	−0.625	0.370	−0.536	−0.791
(0.75,0.75,0.0)	−0.639	0.323	−0.451	−0.767

TABLE V. Anharmonic contributions to constant-volume specific heat, at room temperature. The units are Joule$\cdot$K^{-1}mol^{-1}. (a) The calculation is carried out on the base of Eqs. (11) and (12). (b) The calculation is based on Eq. (13); diagrams in Fig. 6 have been evaluated.

	ΔC_V^{anh}(a)	ΔC_V^{anh}(b)
Cu		-0.44
Ag	-0.52	-0.85
Au	-0.61	-0.97

shows that, to first order at temperatures $T > \Theta_D$,

$$\Delta S^{\text{anh}} = \Delta C_V^{\text{anh}} , \tag{12}$$

where ΔS^{anh} is the anharmonic contribution to entropy. The experimental Debye temperature (at $T=0$) is higher than room temperature in Cu and lower than room temperature in Ag and Au.[30] It follows that Eq. (12) can be correctly used to evaluate the room-temperature value of ΔC_V^{anh} only for Ag and Au. Then we have replaced the harmonic frequencies $\omega_0(\mathbf{q},j)$ in Eq. (11) by

$$\omega_0(\mathbf{q},j) + \Delta^{(3)}(\mathbf{q},j) + \Delta^{(4)}(\mathbf{q},j)$$

and, on the base of Eq. (12), ΔC_V^{anh} as been evaluated at room temperature. The results are given in Table V. A negative anharmonic contribution to constant-volume specific heat is found in both metals.

ΔC_V^{anh} can also be related to the perturbative term in the Helmholtz free energy F_1^{anh} according to the definition

$$\Delta C_V^{\text{anh}} = -T \left[\frac{\partial^2 F_1^{\text{anh}}}{\partial T^2} \right]_V . \tag{13}$$

Direct evaluation of the low-order diagrams in F_1^{anh} [see Figs. 6(a) and 6(b)], allows one to determine ΔC_V^{anh} by Eq. (13). This exact procedure had already been applied in the case of copper.[13] We have carried out the calculations also for Ag and Au. The results are in good agreement with those obtained by Eq. (12), as Table V shows. Our theoretical estimates therefore support the conclusion of Martin.[15]

V. CONCLUSIONS

Let us summarize the main results of this work. Anharmonic lattice vibrations in noble metals have been studied in detail. In these systems, the interatomic forces are known to be very complicated and simple pseudopotential theories are inadequate to deal with relevant many-body effects. We have adopted a force-constant-model potential which parametrizes the most important harmonic and anharmonic interactions. General relations between the anharmonic force constants and the higher-order elastic constants have been derived. Since the force constants are fitted to experimental data (phonon frequencies and elastic constants), the electronic contributions are also incorporated.

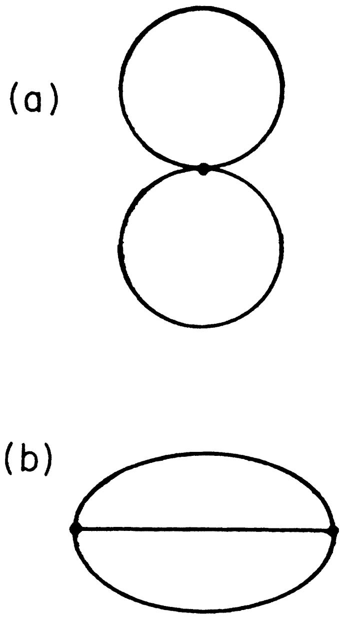

FIG. 6. (a) First-order diagram contributing to C_V^{anh}. (b) Second-order diagram contributing to C_V^{anh}.

A many-body approach which allows one to include the volume dependence of the Helmholtz free energy has been used to calculate the thermoelastic properties in a wide range of temperatures. We have shown that the cubic anharmonic interactions have to be extended up to the third-neighbor shell, in order to fit the experimental data in Ag and Au. In this context, copper exhibits a relatively simpler behavior than silver and gold. Some discrepancies still remain for silver, probably due to the limited accuracy of the experimental elastic constants data which have been used.

Microscopic anharmonic effects, markedly the line shifts, have been computed within low-order perturbation theory at room temperature. We have found that the major contribution to phonon frequency shifts Δ_T is due to the volume-dependent term $\Delta^{(0)}$. Therefore, a correct evaluation of the thermal expansion linear coefficient is essential in order to estimate Δ_T accurately. A good agreement between theory and experiment is found in copper for which high-temperature experimental data are available. The lowest-order terms in the real part of phonon self-energy tend to cancel each other. However, this cancellation does not take place for longitudinal phonons along the $[\xi,0,0]$ direction (at $\xi=0.6$ in Au and at $\xi=0.8$ in Cu and Ag) and an enhanced line shift appears. To our knowledge, experimental evidence for this feature has not been provided, but we would emphasize that a similar behavior was found in aluminum by other investigators.

Finally, we have computed the anharmonic contribution to constant-volume specific heat (ΔC_V^{anh}) at room temperature. ΔC_V^{anh} has been evaluated by the harmonic entropy formula, after replacing the harmonic frequencies with the renormalized frequencies at constant volume. Alternatively, the lowest-order diagrams in the anharmonic Helmholtz free energy, which contribute to ΔC_V^{anh}, have been calculated. Both of the approaches yield a slightly negative sign for ΔC_V^{anh}, in agreement with the suggestions of recent experimental analyses. The sign of ΔC_V^{anh} is critically determined by the values of cubic and quartic anharmonic force cosntants. Therefore, our results indicate that the whole treatment of anharmonic lattice vibrations in noble metals has been carried out with a good accuracy.

ACKNOWLEDGMENTS

I wish to thank Professor V. Bortolani for useful suggestions and S. Kilimann for her kind collaboration. Part of this work has been carried out at the Department of Physics, University of Florence (Florence, Italy).

APPENDIX A

The energy density u^e due to a homogeneous deformation is given by[31]

$$
\begin{aligned}
u^e &= u_1^e+u_2^e+u_3^e+u_4^e \ , \\
u_1^e &= \sum_{\alpha,\beta} C_{\alpha\beta}\epsilon_{\alpha\beta} \ , \\
u_2^e &= \tfrac{1}{2}\sum_{\alpha,\beta,\gamma,\delta}(C_{\alpha\beta,\gamma\delta}+C_{\beta\delta}\delta_{\alpha\gamma})\epsilon_{\alpha\beta}\epsilon_{\gamma\delta} \ , \\
u_3^e &= \tfrac{1}{6}\sum_{\alpha,\beta,\gamma,\delta,\xi,\mu}(C_{\alpha\beta,\gamma\delta,\xi\mu}+C_{\alpha\beta,\delta\mu}\delta_{\gamma\xi}+C_{\beta\mu,\gamma\delta}\delta_{\alpha\xi}+C_{\beta\delta,\xi\mu}\delta_{\alpha\gamma})\epsilon_{\alpha\beta}\epsilon_{\gamma\delta}\epsilon_{\xi\mu} \ , \\
u_4^e &= \tfrac{1}{24}\sum_{\substack{\alpha,\beta,\gamma,\delta,\\ \xi,\mu,\nu,\tau}}(C_{\alpha\beta,\gamma\delta,\xi\mu,\nu\tau}+C_{\beta\delta,\xi\mu,\nu\tau}\delta_{\alpha\gamma}+C_{\beta\mu,\gamma\delta,\nu\tau}\delta_{\alpha\xi}+C_{\beta\tau,\gamma\delta,\xi\mu}\delta_{\alpha\nu} \\
&\qquad +C_{\alpha\beta,\delta\mu,\nu\tau}\delta_{\xi\gamma}+C_{\alpha\beta,\xi\mu,\delta\tau}\delta_{\nu\gamma}+C_{\alpha\beta,\gamma\delta,\mu\tau}\delta_{\xi\nu}+C_{\beta\delta,\mu\tau}\delta_{\gamma\alpha}\delta_{\nu\xi}+C_{\beta\mu,\delta\tau}\delta_{\xi\alpha}\delta_{\nu\gamma}+C_{\beta\tau,\mu\delta}\delta_{\nu\alpha}\delta_{\gamma\xi})\epsilon_{\alpha\beta}\epsilon_{\gamma\delta}\epsilon_{\xi\mu}\epsilon_{\nu\tau} \ ,
\end{aligned} \tag{A1}
$$

where $\epsilon_{\alpha\beta}$ is the strain-rotation tensor, $C_{\alpha\beta,\gamma\delta}$, $C_{\alpha\beta,\gamma\delta,\xi\mu}$, and $C_{\alpha\beta,\gamma\delta,\xi\mu,\nu\tau}$ are the second-, third-, and fourth-order elastic constants, respectively.

If we restrict ourselves to consider pairwise anharmonic interactions, the cubic and quartic terms in the potential energy of a fcc crystal can be written in the following form:

$$
\begin{aligned}
\phi_3 &= \tfrac{1}{12}\sum_i \sum_{L,L'} \sum_{\alpha,\beta,\gamma} \phi^{(i)}_{\alpha\beta\gamma}(L,L')u_\alpha(L,L')u_\beta(L,L')u_\gamma(L,L') \ , \\
\phi_4 &= \tfrac{1}{48}\sum_i \sum_{L,L'} \sum_{\alpha,\beta,\gamma,\delta} \phi^{(i)}_{\alpha\beta\gamma\delta}(L,L')u_\alpha(L,L')u_\beta(L,L')u_\gamma(L,L')u_\delta(L,L') \ ,
\end{aligned} \tag{A2}
$$

with $u_\alpha(L,L')\equiv u_\alpha(L)-u_\alpha(L')$, $u_\alpha(L)$ is the Cartesian component of the phonon displacement field. Once a homogeneous deformation is applied to the crystal, $\mathbf{u}(L)$ is related to the atomic mean position $\mathbf{R}(L)$ by

$$
u_\alpha(L)=\sum_\beta(\delta_{\alpha\beta}+\epsilon_{\alpha\beta})R_\beta(L) \ . \tag{A3}
$$

In Eqs. (A2), the index i specifies the interaction between ith neighbors. It should be emphasized that the sums over the atomic sites L,L' must be consistent with the index i. $\phi^{(i)}_{\alpha\beta\gamma}(L,L')$ and $\phi^{(i)}_{\alpha\beta\gamma\delta}(L,L')$ are the third- and fourth-order force-constant tensors whose explicit expressions are

$$
\begin{aligned}
\phi^{(i)}_{\alpha\beta\gamma}(L,L') &= \frac{1}{r_i^4}\left[r_i\phi'''(r_i)-3\phi''(r_i)+\frac{3}{r_i}\phi'(r_i)\right]R_\alpha(L,L')R_\beta(L,L')R_\gamma(L,L') \\
&\quad +\frac{1}{r_i^2}\left[\phi''(r_i)-\frac{1}{r_i}\phi'(r_i)\right][R_\alpha(L,L')\delta_{\beta\gamma}+R_\beta(L,L')\delta_{\alpha\gamma}+R_\gamma(L,L')\delta_{\alpha\beta}] \ , \\
\phi^{(i)}_{\alpha\beta\gamma\delta}(L,L') &= \frac{1}{r_i^6}\left[r_i^2\phi''''(r_i)-6r_i\phi'''(r_i)+15\phi''(r_i)-\frac{15}{r_i}\phi'\right]R_\alpha(L,L')R_\beta(L,L')R_\gamma(L,L')R_\delta(L,L') \\
&\quad +\frac{1}{r_i^4}\left[r_i\phi'''(r_i)-3\phi''(r_i)+\frac{3}{r_i}\phi'(r_i)\right] \\
&\quad \times[\delta_{\alpha\beta}R_\gamma(L,L')R_\delta(L,L')+\delta_{\alpha\gamma}R_\beta(L,L')R_\delta(L,L')+\delta_{\alpha\delta}R_\gamma(L,L')R_\beta(L,L') \\
&\qquad +\delta_{\gamma\beta}R_\alpha(L,L')R_\delta(L,L')+\delta_{\delta\beta}R_\gamma(L,L')R_\alpha(L,L')+\delta_{\gamma\delta}R_\alpha(L,L')R_\beta(L,L')] \\
&\quad +\frac{1}{r_i^2}\left[\phi''(r_i)-\frac{1}{r_i}\phi'(r_i)\right](\delta_{\alpha\beta}\delta_{\gamma\delta}+\delta_{\alpha\gamma}\delta_{\beta\delta}+\delta_{\alpha\delta}\delta_{\gamma\beta}) \ .
\end{aligned} \tag{A4}
$$

r_i is the ith-neighbor distance and $\phi(r)$ is the two-body interatomic potential. We define

$$\begin{aligned} \alpha_i &= \frac{\phi'(r_i)}{r_i} , \\ \beta_i &= \phi''(r_i) , \\ Y_i &= r_i \phi'''(r_i) , \\ Q_i &= r_i^2 \phi''''(r_i) . \end{aligned} \tag{A5}$$

The harmonic force constants α_i and β_i are fitted to the measured phonon frequencies[32-34] and to the second-order elastic constants. Three-body forces have also been included in the harmonic-model potential in order to avoid the fulfillment of second-order Cauchy relations. The effects of strain on the anharmonic potential energy are accounted for once Eq. (A3) is inserted in Eqs. (A2). By equating the cubic potential energy density ϕ_3/V (V is the crystal volume) and the cubic elastic energy density u_3^e, the following relations between the force constants Y_i and the third-order elastic constants are established:[24]

$$\begin{aligned} &\tfrac{1}{2}C_{111}+3C_{112}+C_{123}+\tfrac{3}{2}C_{11}+3C_{12} \\ &\qquad = \frac{1}{a}(2Y_1+2Y_2+12Y_3) , \\ &\tfrac{1}{3}C_{111}+C_{112}+C_{11}+C_{12} = \frac{1}{a}[\tfrac{5}{6}Y_1+\tfrac{4}{3}Y_2+\tfrac{43}{9}Y_3 \\ &\qquad +\tfrac{1}{2}(\beta_1-\alpha_1)+\tfrac{11}{3}(\beta_3-\alpha_3)] , \\ &8C_{456}+6C_{44} = \frac{1}{a}[\tfrac{32}{3}Y_3+6(\beta_i-\alpha_1)+4(\beta_3-\alpha_3)] , \end{aligned} \tag{A6}$$

where a is the lattice constant and the Voigt notation is used for the elastic constants. We emphasize that the third-order Cauchy relations are not violated since the very central forces have been retained in the anharmonic potential. It follows that three out of six third-order elastic constants are independent. Therefore, central cubic interactions have to be extended up to third-neighbor shell and three force constants Y_i $(i=1,2,3)$ can be fitted to the experimentally known third-order elastic constants.[19]

At the fourth order, 4 out of 11 elastic constants are independent, if the Cauchy relations hold. However, to be consistent with the foregoing description of the cubic term, central quartic interactions are also extended up to the third-neighbor shell. By equating the quartic potential-energy density ϕ_4/V and the quartic elastic density u_4^e, the following relations between the force constants Q_i $(i=1,2,3)$ and the fourth-order elastic constants are derived:

$$\begin{aligned} &\tfrac{1}{8}C_{1111}+C_{1112}+\tfrac{3}{4}C_{1122}+\tfrac{3}{2}C_{1123}+\tfrac{3}{4}C_{111}+\tfrac{9}{2}C_{112}+\tfrac{3}{2}C_{123}+\tfrac{1}{6}C_{11}+\tfrac{3}{4}C_{12} = \frac{1}{a}(\tfrac{1}{2}Q_1+\tfrac{1}{2}Q_2+3Q_3) , \\ &\tfrac{1}{12}C_{1111}+\tfrac{1}{3}C_{1112}+\tfrac{1}{4}C_{1122}+\tfrac{1}{2}C_{111}+\tfrac{3}{2}C_{112}+\tfrac{1}{4}C_{11}+\tfrac{1}{4}C_{12} = \frac{1}{a}[\tfrac{3}{16}Q_1+\tfrac{1}{3}Q_2+\tfrac{211}{216}Q_3+\tfrac{1}{8}Y_1+\tfrac{47}{36}Y_3 \\ &\qquad -\tfrac{3}{16}(\beta_1-\alpha_1)-\tfrac{169}{72}(\beta_3-\alpha_3)] , \\ &\tfrac{1}{24}C_{1111}+\tfrac{1}{4}C_{111}+\tfrac{1}{8}C_{11} = \frac{1}{a}[\tfrac{1}{48}Q_1+\tfrac{1}{6}Q_2+\tfrac{43}{216}Q_3+\tfrac{1}{8}Y_1+\tfrac{23}{36}Y_3-\tfrac{3}{16}(\beta_1-\alpha_1)-\tfrac{73}{72}(\beta_3-\alpha_3)] . \end{aligned} \tag{A7}$$

The complete set of fourth-order elastic constants has been measured only for copper.[35] As for silver and gold, some estimates of the leading fourth-order elastic constants have been provided[20,36] by assuming the validity of the Cauchy relations. The force constants Q_i $(i=1,2,3)$ have been fitted to these available data. In our previous paper,[13] an equation which relates the leading force constant Q_1 to the strain derivative of the Grüneisen parameter has been obtained. We report it here

$$Q_1 = \left[3 \left(\frac{\partial \ln \gamma_{\rm td}}{\partial \ln V} \right)_T + \frac{g}{f} \right] \frac{g}{12} - 2Y_1 + 4(\beta_1-\alpha_1) \tag{A8}$$

with

$$\begin{aligned} f &= \sum_i N_i(\beta_i+2\alpha_i) , \\ g &= 12[Y_1+2(\beta_1-\alpha_1)] . \end{aligned} \tag{A9}$$

N_i is the number of atoms in the ith-neighbor shell.

If the long-range force constants $(i \geq 2)$ are dropped in Eqs. (A7), each of Eqs. (A7) should yield a value of Q_1 consistent with that obtained from Eq. (A8). We have checked that this consistency holds for all the noble metals. In calculations of Sec. III, the anharmonic interactions are extended up to third neighbor and, therefore, the Q_i $(i=1,2,3)$ as given from the system of Eqs. (A7) have been used.

APPENDIX B

In quasiharmonic approximation the stress tensor $\sigma_{\alpha\beta}$ can be written as follows:

$$V\sigma_{\alpha\beta}(T)=-\sum_{\mathbf{q},j}\gamma_{\alpha\beta}(\mathbf{q},j)\hbar\omega(\mathbf{q},j)(n_{\mathbf{q}j}+\tfrac{1}{2}) , \tag{B1}$$

where $\gamma_{\alpha\beta}$ is the Grüneisen tensor. By evaluating the diagram $D1$ in Fig. 1, an explicit expression for the stress tensor can be obtained [see Eqs. (7) and (A2.1) in Ref. 13]. In cubic crystals, the mode Grüneisen parameter $\gamma(\mathbf{q},j)$ is given by

$$\gamma(\mathbf{q},j)=\tfrac{1}{3}\sum_{\alpha=1}^{3}\gamma_{\alpha\alpha}(\mathbf{q},j) . \tag{B2}$$

By using Eqs. (B1) and (B2), the mode Grüneisen parameter can be linked to the cubic anharmonic force constants. Once the cubic anharmonic forces are extended up to the third-neighbor shell, the following relation holds:

$$\begin{aligned}\gamma(\mathbf{q},j)=-\frac{a}{2M\omega_0^2(\mathbf{q},j)}\Bigg[&\frac{Y_1}{a}A(\mathbf{q},j)+\frac{Y_2}{a}C(\mathbf{q},j)+\frac{Y_3}{a}E(\mathbf{q},j)+\frac{\beta_1-\alpha_1}{a}[2B(\mathbf{q},j)-3A(\mathbf{q},j)]\\&+\frac{\beta_2-\alpha_2}{a}D(\mathbf{q},j)+\frac{\beta_3-\alpha_3}{a}[F(\mathbf{q},j)-3E(\mathbf{q},j)]\Bigg] ,\end{aligned} \tag{B3}$$

where M is the atomic mass and

$$\begin{aligned}
A(\mathbf{q},j)&=(1-c_xc_y)(e_x^2+e_y^2)+(1-c_xc_z)(e_x^2+e_z^2)+2s_xs_y\cdot e_xe_y+2s_xs_z\cdot e_xe_z ,\\
B(\mathbf{q},j)&=(2-c_xc_y-c_xc_z)(3e_x^2+e_y^2+e_z^2)+2s_xs_y\cdot e_xe_y+2s_xs_z\cdot e_xe_z ,\\
C(\mathbf{q},j)&=2e_x^2(1-c_{2x}) ,\\
D(\mathbf{q},j)&=2(e_y^2+e_z^2)(1-c_{2x}) ,\\
E(\mathbf{q},j)&=\tfrac{4}{9}\{e_x^2\cdot[8(1-c_{2x}c_yc_z)+\tfrac{1}{2}(2-c_xc_{2y}c_z-c_xc_yc_{2z})]\\
&\quad+e_y^2\cdot[2(2-c_{2x}c_yc_z-c_xc_{2y}c_z)+\tfrac{1}{2}(1-c_xc_yc_{2z})]+e_z^2\cdot[2(2-c_{2x}c_yc_z-c_xc_yc_{2z})+\tfrac{1}{2}(1-c_xc_{2y}c_z)]\\
&\quad+2e_xe_y\cdot(4s_{2x}s_yc_z+s_xs_{2y}c_z+\tfrac{1}{2}c_xs_ys_{2z})+2e_xe_z\cdot(4s_{2x}s_zc_y+s_xs_{2z}c_y+\tfrac{1}{2}c_xs_zs_{2y})\\
&\quad+2e_ze_y\cdot(2s_{2x}s_zc_y+c_xs_{2y}s_z+c_xs_ys_{2z})\} ,\\
F(\mathbf{q},j)&=\tfrac{4}{3}\{(3e_x^2+e_y^2+e_z^2)[4(1-c_{2x}c_yc_z)+(2-c_xc_{2y}c_z-c_xc_yc_{2z})]\\
&\quad+2e_xe_y\cdot(s_{2z}s_yc_x+2s_xs_{2y}c_z+2s_{2x}s_yc_z)+2e_xe_z\cdot(s_{2y}s_zc_x+2s_xs_{2z}c_y+2s_{2x}s_zc_y)\} ,
\end{aligned} \tag{B4}$$

with $c_\alpha=\cos(\pi q_\alpha)$, $s_\alpha=\sin(\pi q_\alpha)$, $c_{2\alpha}=\cos(2\pi q_\alpha)$, $s_{2\alpha}=\sin(2\pi q_\alpha)$, $e_\alpha\equiv e_\alpha(\mathbf{q},j)$ is the Cartesian component of the polarization vector ($\alpha=x,y,z$).

From Eqs. (5), (B1), and (B2), the thermal pressure $\alpha\cdot B^T$ can be easily written as

$$\alpha B^T=\frac{T^{-1}\beta\hbar^2}{V}\sum_{\mathbf{q},j}\gamma(\mathbf{q},j)\omega_0^2(\mathbf{q},j)n_{\mathbf{q},j}(n_{\mathbf{q},j}+1) , \tag{B5}$$

where the temperature derivative of the Bose-Einstein factor has been used.

---

*Present address: Institut für Theoretische Physik, Jungiusstrasse 9, D-2000 Hamburg 36, West Germany.

[1] A. A. Maradudin, Phys. Status Solidi **2**, 1493 (1962).

[2] A. A. Maradudin and A. E. Fein, Phys. Rev. **128**, 2589 (1962).

[3] M. L. Klein and J. L. Horton, J. Low Temp. Phys. **9**, 151 (1972).

[4] M. L. Klein, J. L. Horton, and J. L. Feldman, Phys. Rev. **184**, 968 (1969).

[5] H. Falk, Am. J. Phys. **38**, 858 (1970).

[6] N. R. Werthamer, Phys. Rev. B **1**, 572 (1970).

[7] V. G. Vaks, S. P. Kravchuk, and A. V. Trefilov, J. Phys. F **10**, 2325 (1980).

[8] H. R. Glyde, J. P. Hansen, and M. L. Klein, Phys. Rev. B **16**, 3476 (1977).

[9] R. M. MacDonald, R. D. Mountain, and R. C. Shukla, Phys. Rev. B **20**, 4012 (1979).

[10] J. Rosèn and G. Grimvall, Phys. Rev. B **27**, 7199 (1983).

[11] T. H. K. Barron, in *Lattice Dynamics*, edited by R. F. Wallis (Pergamon, Oxford, 1965).

[12] J. C. K. Hui and P. B. Allen, J. Phys. C **8**, 2923 (1975).

[13] M. Zoli and V. Bortolani, J. Phys. Condens. Matter **2**, 525 (1990).

[14] T. H. K. Barron and M. L. Klein, in *Dynamical Properties of Solids*, edited by G. K. Horton and A. A. Maradudin (North-

Holland, Amsterdam, 1974).
[15] D. L. Martin, Can. J. Phys. **65**, 1104 (1987).
[16] A. Larose and B. N. Brockhouse, Can. J. Phys. **54**, 1990 (1976).
[17] R. A. MacDonald and W. M. MacDonald, Phys. Rev. B **24**, 1715 (1981).
[18] G. D. Mahan, *Many Particle Physics* (Plenum, New York, 1981).
[19] Y. Hiki and A. V. Granato, Phys. Rev. **144**, 411 (1966).
[20] Y. Hiki, J. F. Thomas, and A. V. Granato, Phys. Rev. **153**, 764 (1967).
[21] T. A. Hahn, J. Appl. Phys. **41**, 5096 (1970).
[22] Y. S. Touloukian, R. K. Kirby, R. E. Taylor, and T. Y. Lee, *Thermophysical Properties of Matter* (IFI/Plenum, New York, 1970), Vols. 4 and 12.
[23] T. R. Koehler, N. S. Gillis, and D. C. Wallace, Phys. Rev. B **1**, 4521 (1970).
[24] M. Zoli, G. Santoro, V. Bortolani, A. A. Maradudin, and R. F. Wallis, Phys. Rev. B **41**, 7507 (1990).
[25] W. Cochran and R. A. Cowley, *Handbook der Physik* (Springer-Verlag, Berlin, 1967).
[26] G. Gilat and R. M. Nicklow, Phys. Rev. **143**, 487 (1966).
[27] R. Stedman, L. Almquist, and G. Nilsson, Phys. Rev. **162**, 549 (1967).
[28] G. Leibfried and W. Ludwig, in *Solid State Physics,* edited by F. Seitz and D. Turnbull (Academic, New York, 1961), Vol. 12.
[29] A. J. Leadbetter, J. Phys. C **1**, 1489 (1968).
[30] D. L. Martin, Phys. Rev. **170**, 650 (1968).
[31] R. A. Coldwell-Horsfall, Phys. Rev. **129**, 22 (1963).
[32] G. Nilsson and S. Rolandson, Phys. Rev. B **9**, 3278 (1974).
[33] W. A. Kamitakahara and B. N. Brockhouse, Phys. Lett. **29A**, 639 (1969).
[34] J. W. Lynn, H. G. Smith, and R. M. Nicklow, Phys. Rev. B **8**, 3493 (1973).
[35] H. Soma and Y. Hiki, J. Phys. Soc. Jpn. **37**, 544 (1974).
[36] M. F. Rose, Phys. Status Solidi **17**, K199 (1966).